

Integrating IoT with LQR-PID controller for online surveillance and control of flow and pressure in fluid transportation system

E.B. Priyanka^{a,*}, C. Maheswari^a, S. Thangavel^a, M. Ponni Bala^b

^a Department of Mechatronics Engineering, Kongu Engineering College, Perundurai, Erode, India

^b Department of Electronics and Instrumentation Engineering, Kongu Engineering College, Perundurai, Erode, India



ARTICLE INFO

Keywords:

Integrated IoT architecture
Fluid transportation system
Automation and control system
IoT module

ABSTRACT

In the modern upgradation era, monitoring and control system is essential to ensure the smooth operation of the long-distance pipeline in the fluid transportation system. Now-a-days, to design an accurate online monitoring and control system represents a critical task that requires proactive planning in fluid transportation system. In the fluid pipeline system, the huge amount of fluid loss caused by leakages, cracks and blockages due to extreme pressure changes in the pipelines during transportation. The present research work focuses on developing Integrated IoT based intelligent architecture to perform online monitoring and control of pressure and flow rate in the fluid transportation system. The proposed Integrtaed IoT based architecture holds SCADA with LQR-PID controller as local control unit or local intelligence. During crack and leak occurrences in the fluid pipeline, SCADA with PID controller cannot afford desired control action due to drastic change in the pressure and the flow rate. Hence the entire architecture is monitored and accessed through high-level online server IoT interface to identify leaks and cracks in the pipeline at the initial stage before it leads to any catastrophic situations. In order to attain better data communication between cloud server and pipeline hardware setup, smart IoT module is designed and fabricated. Once the crack or leaks is identified in the IoT front end, immediately emergency shut off is activated by the cloud server through smart IoT module by stopping the pump. The developed Integrated IoT architecture is experimentally validated in real-time lab-scale fluid transportation pipeline system. Further in this present work, the performance of Linear Quadratic Regulator-PID controller to regulate pressure and flow rate of the fluid being transported is analyzed by comparing with convnetional controllers like Internal-Mode controller and Zigler-Nichols controller.

1. Introduction

Nowadays, fluid transportation system require a more reliable, accurate, robust and efficient control system for detecting leaks, cracks or bursts over the pipeline system. As of now, Indian Fluid Corporation Limited technologically upgraded pipelines in India with the help of Supervisory Control and Data Acquisition (SCADA) framework to continually monitor the mobilization of fluid products through the pipeline [1]. SCADA system is a software package positioned on top of hardware and is interfaced with industrial processing units through Programmable Logic Controllers (PLC) or Remote Terminal Unit (RTU) which performs monitoring and control process for the entire fluid pipeline systems [3,4]. Meanwhile SCADA system alone are not suitable for central monitoring and control of entire pipeline system. Because it holds limitations such as not scalable due to slow data processing with minimum memory storage and non-feasible when the software or

protocol upgradation availability resulting in high maintenance cost [2]. Consequently, wireless networks can be considered as one of the suitable solutions in harsh environments, and employing IoT can overcome the foregoing limitations. Industrial Internet of Things is investigated towards the development of inspection technique to detect the risk occurrences incorporated with hardware system. In this context, all modernized industries have been undertaken the Internet of Things (IoT) platform synchronizing communication between the hardware elements (sensors, actuators, control panel, etc.) and networked embedded data devices [35–37].

[40] conducted an experiment using IoT embedded Linux system to cloud monitoring of the photovoltaic system in real-time by incorporating Raspberry-Pi as the main controller. It exemplifies the multi-user monitoring system with a cloud server through an embedded Linux system of Raspberry-Pi to measure photovoltaic plant voltage, current, temperature, and humidity. The advantage of developed IoT

* Corresponding author.

E-mail address: priyankabhaskaran1993@gmail.com (E.B. Priyanka).

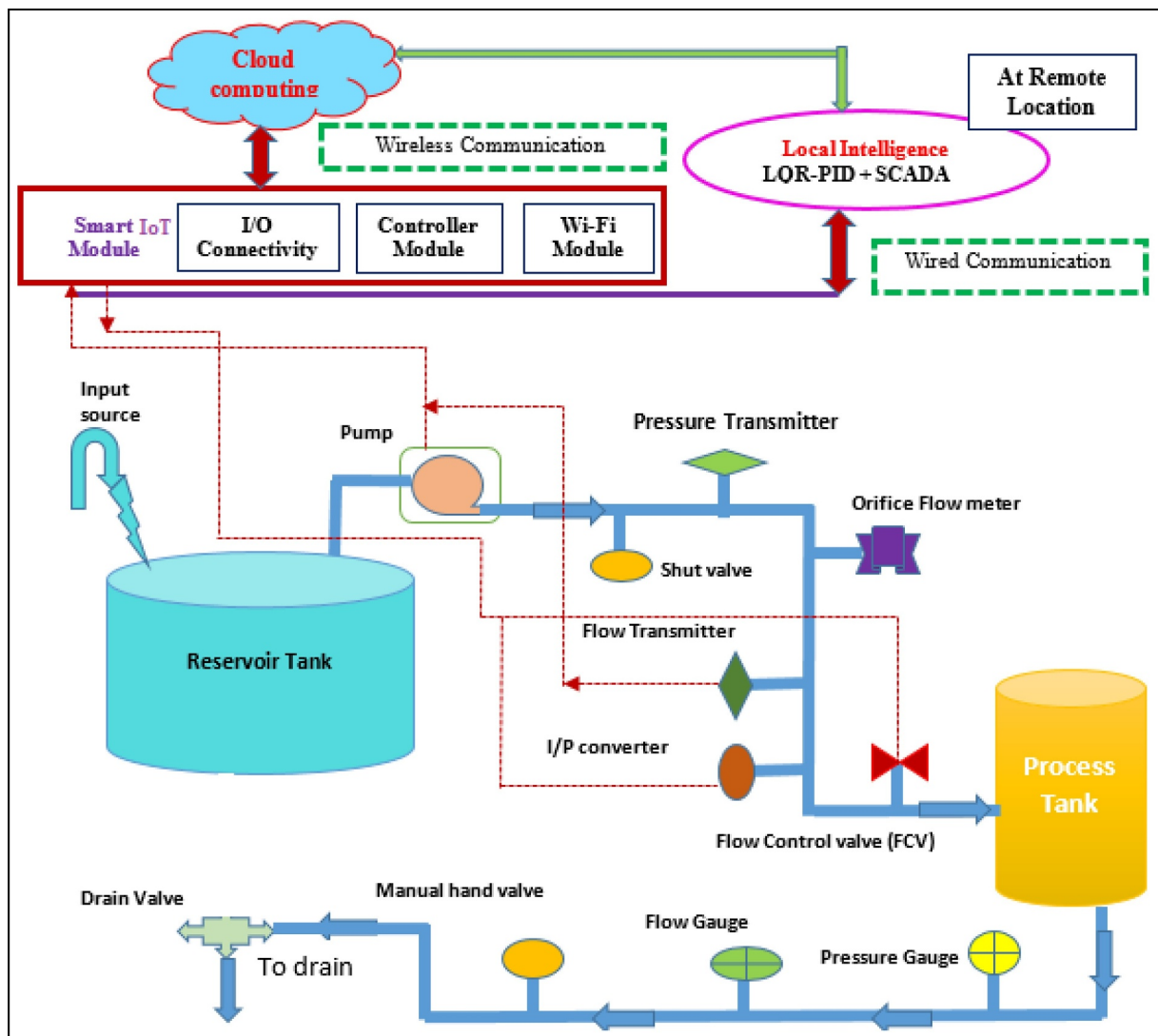


Fig. 1. Integrated IoT architecture with local intelligence (SCADA + LQR-PID).

system is that it reduces the cost of comparing with traditional hardware and software used for monitoring and acquisition process [30–34]. [44] developed an IoT infrastructure for making intelligent and productive transportation system in smart cities for enhanced industrial integration. The designed intelligent transportation system is experimentally tested in city vehicle transport system and the operating system runs on the Java IDE platform [5].

Li et al. proposed a cascade control system to function in IoT circumstance without any application of a special instrument server [30]. It cascades level and flow processes individually by implementing Particle Swarm Optimized (PSO) PID controllers. The IoT communication is made feasible by allowing on-ship microcontroller supported with Wide Area Network (WAN) which receives data from flow and level transmitter respectively [6]. [43] explained the application of industrial IoT in the elevator system [31]. The developed IoT architecture mainly depicts its importance in water distribution and oil, gas distribution network separately. The main insight is to improve the monitoring process and allow a real time management and data processing [7,8]. Yong conducted experimentation using Advanced Meters Infrastructure (AMI) based on the Internet of Things with three different categories of communications. It applies the main focuses on communication between meters and utilizing server by meter access, meter gateway, and new cellular technology [34].

The undertaken pioneering works related to IoT based application

shows the modification in the control techniques and data communication link involved in the application layer based on the experimenting system characterizations. Therefore for the fluid transportation system, the present work describes the innovative technique of Integrated IoT based intelligent monitoring and control framework to enhance performance of existing SCADA based remote monitoring and control. The Integrated IoT architecture incorporates SCADA with LQR (Linear Quadratic Regulator)-PID controller as a Local Control Unit (LCU). The entire fluid pipeline system is governed by the IoT technology and operated via high-level secured IoT front end interface which is manageable from online server at any time. A smart IoT module is designed to serve as a platform between the experimental hardware and the IoT front end interface to make appropriate decisions during leaks and cracks by abnormal pressure and flow rate changes. The structure of the paper is described as follows:

1. Design and development of Integrated IoT based intelligent monitoring and control architecture for fluid pipeline transportation system.
2. Establishment of lab-scale experimental hardware setup with SCADA.
3. Performance analysis of local monitoring and control of fluid transport system using local intelligence holding SCADA with LQR-PID controller.

4. Development of smart IoT module with high level secured IoT front end interface with emergency shut-off during crack and leakages in the fluid pipeline.
5. Real-time implementation of developed Integrated IoT based architecture for online monitoring and control of pressure and flow rate in the experimental lab-scale fluid transportation setup.

2. Proposed integrated IoT based architecture

The proposed integrated IoT architecture enhances existing application layer by incorporating a centralized cloud server with local intelligence for better data analysis and storage. The developed application layer exhibits the data analysis with monitoring and control application. So, the local intelligence performs at the field station when the field parameters variation is under normal operating threshold ranges. During risk circumstance caused by abnormal variation in the field parameters, immediately merged cloud computing techniques afford enlightened online monitoring and control at a specified time. It is accomplished by designing SCADA with LQR-PID controller as local intelligence and cloud server as a centralized database along with cloud computing techniques to proactively decide and react in a timely manner. The data processing algorithms running on stored cloud data will perform online control actions (fire alerts, shut down of different equipment, identifying the exact location and rectifying the fault, operator alerts) against anomalous events like oil pipeline crack, bursts, etc. A complete redesigned Integrated IoT architecture with local intelligence(SCADA + LQR-PID) for the lab scale experimental for remote monitoring and control of fluid transport pipeline is shown in Fig. 1.

Fig. 1 represents the visualization of the sensors and actuators positioned [7] with the piping having directional tracks of their controls. A real-time pump status, pressure and flow rate sensors data which are regulated by the developed local intelligence (SCADA + LQR-PID) are given to the fabricated smart module which comprises of I/O connectivity, controller and Wi-Fi module. This smart module will uphold the received input and push that to the cloud. In the cloud-centric storage, these sensor data will be updated frequently and it will put to data analytics in order to monitor the fluid transportation through pipelines is sustained within normal operating range. Based on data processing algorithms inferences, generates proper control information to take important decisions against anomalous events, web server IoT interface is exploited to facilitate the decision-making practice. It consists of SCADA at the field control along with data monitoring to process and analyze the situation based on the acquired pressure and flow sensor field data. When the collected data is analyzed and preferred actuation is performed by controlling the actuators without human intervention. During risk occurrences like crack and leaks in the pipeline, the corresponding pump is switched off automatically by triggering required port of the smart IoT module by the online cloud server.

3. LAB scale experimental setup of fluid transport system

The complete experimental setup of fluid transport system is shown in Fig. 2 with the total length of 15 m holding metal pipe of one-inch diameter. The hardware setup comprises of an centrifugal electric pump of 1 hp (horse power), differential pressure transmitter holding a range of 03–15 psi ($0.1\text{--}3 \text{ kg/cm}^2$), and orifice flow meter having the limit of 0–1800 lph (liters per hour) controlled by flow control valve with I/P converter. When the fluid starts to pass through the pipelines, both pressure and flow transmitter simultaneously sends the analog current output signal of 4–20 mA to the main control unit. The pressure and flow rate data are send to the I/O hub module through Centum/Ip net protocol using DCS software platform and also to the smart IoT module for data analysis and storage in the cloud server. Based on these two transmitter readings during transportation, LQR-PID controller in SCADA engineering station sends control signals to the respective I/P converter of flow control valve remotely. The received control signal of

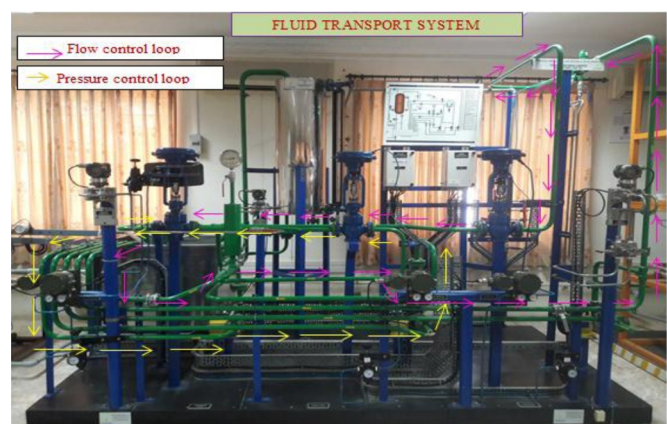


Fig. 2. The lab scale experimental setup of the fluid transport system.

analog current with the range of 4–20 mA is fed into flow I/P converter which converts to calibrated pressure signal. A corresponding pressure signal is fed to the control valve to adjust its operations of opening and closing of control valves until the oil reaches the process tank. For manual inferences, pressure gage displays the pressure in bar scale readings along with positioning manual hand valve and drain valve inappropriate location for safe transportation. The corresponding sensors and actuators specification details of the lab-scale experimental setup is described as follows:

The SCADA incorporating an LQR-PID controller is developed for the experimental setup of the fluid transport system to deal with local monitoring and control of entire pipeline with interface displays for flow rate and its respective pressure monitoring/control panel as shown in Fig. 3. The developed SCADA provides more functional utility options like system message banner, graphic view with graphics and control attributes, trend view, browser bar and tuning window [13].

4. Performance analysis of local intelligence

4.1. Model identification of fluid transport system for pressure and flow rate

4.1.1. Open loop response analysis

For modeling the fluid transport system, a transient response curve is recorded by adjusting the control valve opening in order to acquire the equivalent pressure and flow rate changes of the transporting oil in the open loop structure [9]. This open loop experimentation reveals when the opening of the control valve is around 10% of the overall opening, it possess minimum pressure with maximum flow rate and vice versa when the control valve opening reaches its full stretch of 100%.

The open loop response analysis is carried out by linearly adjusting the percentage of control valve opening. The experimental analysis call-ups with the initial flow rate of 179 lph and pressure of 2.2 kg/cm^2 and continuous readings were documented until the flow rate and pressure influences constant state. The result reveals that for 100% control valve opening the ultimate flow rate and pressure accomplished are 1792 lph and 0.22 kg/cm^2 . Open loop readings were noted for the percentage of control valve opening versus flow rate and pressure conducted through SCADA engineering station is displayed in Fig. 4. The obtained pressure and flow rate data are presented in Table 1 by which the first order model parameters (process gain k_p and process time constant τ_p) are calculated. The evaluated model parameters for pressure and flow rate are given in Table 2. To enumerate first-order structures such as process gain k_p , process time constant τ_p and time delay θ , with

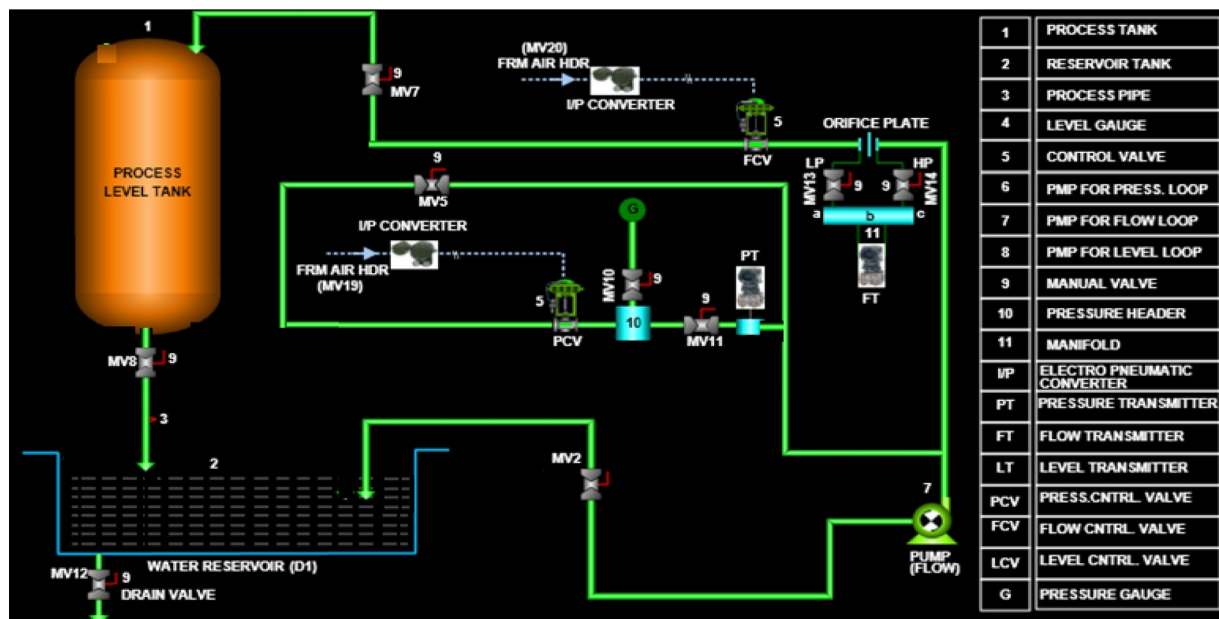


Fig. 3. SCADA view of the lab scale experimental fluid transport system.

[Initial pressure range – Final attained pressure range]

$$k_p = \frac{ / [\text{Maximum flow rate range}]}{[\text{Initial control valve opening} - \text{Final level of valve opening}]}$$

/[Maximum level of valve opening]

$$\tau_p = 1.5 * [T_2 - T_1] \quad (1)$$

$$T_1 \text{ at A1} = [\text{Initial pressure rate} - ((\text{initial level of parameter} - \text{final level of parameter}) * 0.632)]$$

$$T_2 \text{ at A2} = [\text{Initial pressure rate} - ((\text{initial level of parameter} - \text{final level of parameter}) * 0.283)]$$

$$\theta = (T_2 - \tau_p) \quad (2)$$

From Table 2, fluid transportation system exhibits nonlinear behavior with stability state. In order to represent the system in mathematical representation, First Order Plus Time Delay (FOPTD) transfer function ($G(s) = \frac{k_p}{\tau_p s + 1} e^{-\theta s}$) is taken to exemplify the pressure and flow rate control of fluid transport system, where k_p = process gain, τ_p = time constant and θ = process delay [10]. Since pressure and flow rate exploits dynamic variation irrespective time due to external

Table 1

Open loop response analyses of pressure and flow for a various percentage opening of the control valve.

| Percentage of control valve opening (in %) | Flow rate (in lph) (liters per hour) | Pressure (in kg/cm ²) |
|--|---|-----------------------------------|
| 10 | 179 | 2.20 |
| 20 | 230 | 1.92 |
| 30 | 373 | 1.83 |
| 40 | 468 | 1.71 |
| 50 | 585 | 1.48 |
| 60 | 757 | 1.21 |
| 70 | 919 | 0.91 |
| 80 | 1137 | 0.55 |
| 90 | 1429 | 0.36 |
| 100 | 1792 | 0.22 |

influences, the worst case model is considered. Since with the leading process gain followed by lowest time constant assures better control response in closed loop action. The recognized FOPTD model for the flow closed loop of fluid transport system is characterized as,

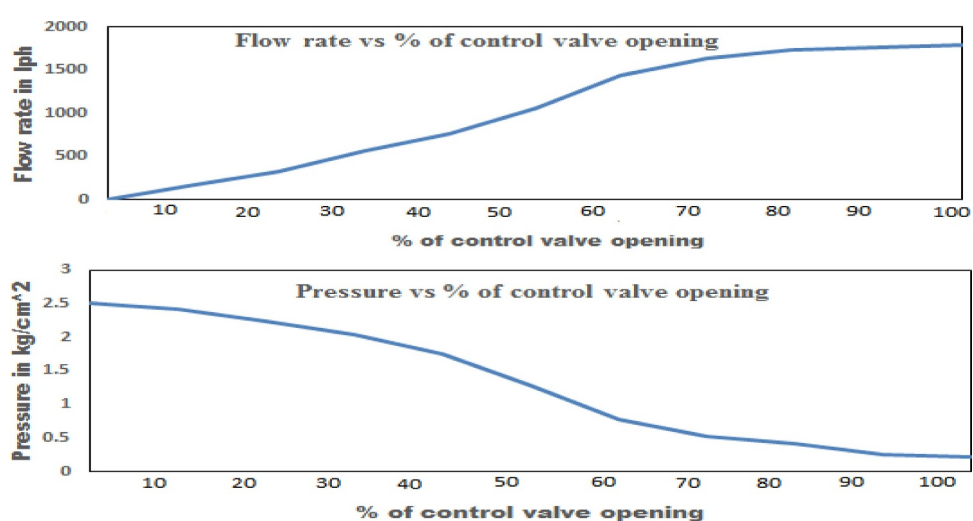


Fig. 4. Pressure and flow rates of the liquid for the different level of control valve opening.

Table 2
Recognized model parameters for various percentage opening of control valve.

| Percentage of control valve opening (%) | Flow rate | | | Pressure | | |
|---|--------------|--------------|-------------|--------------|--------------|--------------|
| | k_p | τ_p (s) | $\theta(s)$ | k_p | τ_p (s) | $\theta(s)$ |
| 20 | 0.329 | 11.941 | 7.91 | 1.681 | 4.95 | 13.58 |
| 40 | 0.485 | 8.317 | 12.83 | 1.364 | 6.43 | 22.84 |
| 60 | 0.914 | 9.084 | 15.72 | 1.649 | 4.026 | 35.59 |
| 80 | 0.046 | 13.51 | 9.89 | 1.024 | 9.88 | 21.91 |
| 100 | 0.871 | 17.46 | 5.16 | 0.995 | 14.32 | 29.92 |

$$G(s) = \frac{0.914}{8.317s + 1} e^{-5.16s} \quad (3)$$

Similarly, the FOPTD model for the pressure closed loop is exemplified as,

$$G(s) = \frac{1.681}{4.026s + 1} e^{-13.58s} \quad (4)$$

The system model identification is arrived by formulated the real-time experimental data obtained from the fluid transport system in open loop performance analysis [11].

4.2. LQR-PID controller design

The undertaken experimental fluid pipeline system resembles as a Single Input Single Output system (i.e. either pressure or flow as input and control valve operation as output), a Linear Quadratic Regulator (LQR) optimal controller can be used due to its fast settling time and effective robustness performances results in practical feedback gains. The LQR method has an efficient procedure for creating controllers for a complex process having tedious control requirements. It makes the designed tuning approach of optimal controller that reduces an oil pipeline system cost function. The cost function is computed by two matrices, Q and R represents the weight of the state vector and the system input respectively. LQR method relies on the state-space model and estimates the optimal control input by resolving the algebraic Riccati Equation. An advanced computation for the selection of Q and R matrices for flow and pressure control process is used by the closed-loop negative feedback system [11]. LQR design approach to obtain optimal control tuning values through the augmented state space description is given by,

$$x(t) = \begin{bmatrix} x_1(t) \\ x_2(t) \\ x_3(t) \end{bmatrix} = \begin{bmatrix} \int_0^t y(t) dt \\ \frac{dy(t)}{dt} \\ y(t) \end{bmatrix} \quad (5)$$

The corresponding differential equation for the state space representation of fluid pipeline system is given with $y(t)$ is an output variable, $x(t)$ is an initial state condition and $u(t)$ is a control variable is given as

$$\frac{dx(t)}{dt} = Ax(t) + Bu(t); y(t) = Cx(t) \quad (6)$$

Where A , B and C are real constant matrices with finite dimensions. The pressure and flow control of an fluid pipeline system is represented in linear constant coefficient differential equation with time period engaged with time delay L

$$\dot{x}(t) = Ax(t) = Bu(t - L) \quad (7)$$

For the fluid pipeline system take control history as $u(t)$ and propagate $x = f(\dot{x}, u, t)$ to develop a state trajectory by forwarding in time [15]. In the case of the linear quadratic regulator with zero terminal cost yields the linear pipeline system dynamic with $L \geq 0$ as

$$L = \frac{1}{2}x^T Q x + \frac{1}{2}u^T R u \quad (8)$$

The PID controller follows corresponding steps to express the LQR, for transforming to the LQR, consider the quadratic performance criterion with a costate cost function

$$J(u(t)) = \frac{1}{2} \sum_0^\infty (x^T(t)Qx(t) + u^T(t)Ru(t)) dt \quad (9)$$

Q is a nonnegative definite matrix that deals with the withdrawal of system states from the equilibrium, and R is a positive definite matrix that tunes the control input. The following LQR design algorithm is used to determine the optimal state feedback ([41]). Consider A , B , C , Q and R specified matrices with suitable dimension, $Q \geq 0$ and $R > 0$, $u(t) = 0$, when $t < 0$. The LQR approach implies that J in Eq. (9) is minimized by the optimal control $u(t)$. When $t \geq L$, this pressure and flow controls system has a possible non zero input signal ([42]). Here L becomes system time delay [12]. Since the hardware setup involves a single-input single-output system with non-linearity behavior, Riccati Equation is considered to compute the control action using $u(t)$. The following LQR design algorithm is used to determine the optimal state feedback.

Step 1: Solve the matrix Algebraic Riccati Equation (ARE)

$$A^T P + PA - PBR^{-1}B^T + QC = 0 \quad (10)$$

Step 2: Determine the optimal state $x^*(t)$ from

$$x^*(t) = [A - BR^{-1}B^T P]x(t) \quad (11)$$

Step 3: Obtain the optimal control $u^*(t)$ from optimal statex $^*(t)$

$$u^*(t) = -R^{-1}B^TPx^*(t) \quad (12)$$

Step 3: Obtain the optimal performance index from

$$J^* = \frac{1}{2}x^{*T}(t)Px(t) \quad (13)$$

The weighting matrices Q and R are important components of an LQR optimization process. The configurations of Q and R features have great influences on system performance. But the selection of matrices Q and R is normally based on an iterative procedure using experimentation carried out on fluid pipeline system ([45]). The transfer function model $G(s) = \frac{b}{s+a}e^{-Ls}$ for the fluid pipeline is represented as $(s+a)e^{-Ls} = -be^{-Ls}u$ which is equivalent to the time-domain equation, $\dot{e} = -ae - bu(t - L)$ for the single-input nonlinear system, the LQR solution for the pipeline system includes

$$u^*(t) = -R^{-1}B^TPx^*(t) \quad (14)$$

where $P = P^T$ denotes a positive value based definite solution in the Riccati Equation. Converting $u^*(t)$ in Eq. (14) back to $u(t)$ in order to obtain a solution to the flow and pressure control is

$$u(t) = \hat{u}(t + L) = -R^{-1}B^TPx(t + L), t \geq 0 \quad (15)$$

From Eq. (15) that the current control $u(t)$ is actually feedback of the future state at the time of $(t + L)$. It confirms that the controller has the prediction capability and may enhance the closed-loop performance compared with conventional LQR or PID design [13]. A PID controller can be represented as

$$u(t) = K_p \left(e(t) + \frac{1}{T_i} \int e(t) dt + \tau_d \frac{de(t)/dt}{dt} \right) = K_p e(t) + K_i \int e(t) dt + K_d de(t)/dt \quad (16)$$

Let $x_1 = \int_0^t e(t) dt$, $x_2 = de(t)/dt$ and $x_3 = e$ such that $x = [x_1 \ x_2 \ x_3]^T$. The Eq. (7) can be written in the following equivalent form:

$$\dot{x} = \begin{bmatrix} 1 & 1 \\ 0 & -a \end{bmatrix} x + \begin{bmatrix} -b \\ -c \end{bmatrix} u(t - L) \quad (17)$$

The estimation of K_p , K_i and K_d tuning values for the SISO system includes comparing Eq. (16) with Eq. (7) yields $\begin{bmatrix} 0 & 1 \\ 0 & -a \end{bmatrix}$; $B = \begin{bmatrix} -b \\ -c \end{bmatrix}$; $C = \begin{bmatrix} 1 & 0 \\ 0 & 1 \end{bmatrix}$ Let $Q = \begin{bmatrix} q_1 & q_2 \\ 0 & q_3 \end{bmatrix}$ and $P = \begin{bmatrix} p_{11} & p_{12} \\ p_{21} & p_{22} \end{bmatrix}$. Substituting into Riccati Eq. (10) gives

$$\begin{aligned} & \begin{bmatrix} 1 & 0 \\ 1 & -a \end{bmatrix} \begin{bmatrix} p_{11} & p_{12} \\ p_{21} & p_{22} \end{bmatrix} + \begin{bmatrix} p_{11} & p_{12} \\ p_{21} & p_{22} \end{bmatrix} \begin{bmatrix} 1 & 0 \\ 1 & -a \end{bmatrix} \\ & - \begin{bmatrix} p_{11} & p_{12} \\ p_{21} & p_{22} \end{bmatrix} \begin{bmatrix} -b \\ -c \end{bmatrix} R^{-1}[-b \quad -c] \begin{bmatrix} p_{11} & p_{12} \\ p_{21} & p_{22} \end{bmatrix} + \begin{bmatrix} q_1 & q_2 \\ 0 & q_3 \end{bmatrix} \begin{bmatrix} 1 & 0 \\ 0 & 1 \end{bmatrix} = 0 \end{aligned} \quad (18a)$$

Its positive definite analytical solutions for Eq. (18a) are

$$\begin{aligned} P_{12} &= \sqrt{q_2 q_3 (R/(b+c))}; P_{22} = -R(a-b) \\ &+ \sqrt{R^2 a^2 + \frac{R b^2 (2p_{12} + q_2)}{b} + \frac{R c^2 (p_{21} + 2q_3)}{c^2}}; \\ P_{11} &= ap_{22} + R^{-1}b^2 p_{21} p_{22} + R^{-2}c^2 p_{12}; \\ P_{21} &= c^2 ap_{12} + \sqrt{q_1 (R/(bc))} (R^{-1}c^2 p_{21} p_{12} + p_{11}) \end{aligned} \quad (18b)$$

Though the control law $\gamma(t)$ given in Eq. (15) is in a time horizon of $t \geq L$, the recovered $u(t)$ actually gives the control signal for operating the control valve in the whole time horizon of $t \geq 0$. $x(t+L)$ is not directly available at time t [14]. However it can be expressed by the transmission of $x(t)$ by Eq. (11) as

$$x(t+L) = e^{A_c x(t)} x(L) \quad (19)$$

The optimal controller in Eq. (19) reduces to

$$u(t) = \begin{cases} -Fe^{A_c t}e^{A(L-t)}x(t), & 0 \leq t < L \\ -Fe^{A_c L}x(t), & L \leq t \end{cases} \quad (20)$$

By optimal control law $u(t) = -Fx(t)$ where F is a gain matrix and substituting this $u(t)$ in Eq. (14) by correlating with Eq. (11) provides

$$\frac{dx(t)}{dt} = (A - BF)x(t) \quad (21)$$

F is a gain matrix obtained from optimal performance index of Eq. (21) after the Laplace transformation to obtain the index as

$$F = R^{-1}[P_{12} \quad P_{22}] \quad (22)$$

The computed closed loop system matrix A_c for fluid transport pipeline system to obtain gain values of PID controller is

$$\begin{aligned} A_c &= A - BF = \begin{bmatrix} 0 & a^2 + (R^{-1}c^2 q_3 + p_{21} q_2 b) p_{12} c \\ -\frac{b^2 (ac^2 + R^{-1}bc + p_{21} p_{22} a^2 c)}{b^2 c} & -R^{-2} a^2 p_{11} \end{bmatrix} \\ &= \begin{bmatrix} 0 & d_1 \\ d_2 & d_3 \end{bmatrix} \end{aligned} \quad (23)$$

To obtain feedback gain, its necessity to calculate $\exp(Ac t)$ using inverse Laplace transformation,

$$\text{Hence } \exp(Ac t) = l^{-1}(sI - Ac)^{-1} \quad (24)$$

After calculating $\exp(Ac t)$ and then multiplying with corresponding gain matrix F of flowrate and pressure, the corresponding LQR optimal tuning value k_p , k_i and k_d for PID controller when $t \geq L$ is estimated as

$$\begin{aligned} K_p(t) &= R^{-1}(b+c)/d_1 d_3, \\ K_i(t) &= R^{-1}c^2 d_2, \\ K_d(t) &= R^{-1}\frac{c}{ba} \left(\frac{d_1 d_2}{d_3} d_1 \right), \end{aligned} \quad (25)$$

4.2.1. LQR PID tuning approach for flow rate control in the fluid transportation system

From the Eq. (3) representing transfer function for a flow control loop, the corresponding values of a , b and c are obtained to form state space matrices as,

$$A = \begin{bmatrix} 0 & 1 \\ 0 & -8.317 \end{bmatrix}; B = \begin{bmatrix} -0.914 \\ -1 \end{bmatrix}; C = \begin{bmatrix} 1 & 0 \\ 0 & 1 \end{bmatrix} \quad (26a)$$

Assigning values for $Q = \begin{bmatrix} q_1 & q_2 \\ 0 & q_3 \end{bmatrix} = \begin{bmatrix} 4.321 & 2.973 \\ 0 & 3.246 \end{bmatrix}$ and $P = \begin{bmatrix} p_{11} & p_{12} \\ p_{21} & p_{22} \end{bmatrix} = \begin{bmatrix} 1.277 & 0.375 \\ 0.293 & 1.342 \end{bmatrix}$; $R = [1 \ 0 \ 0]$ by iterative techniques of conducting experimentation on fluid pipeline system in equilibrium condition [15]. Let the transformed equation for flow control loop is given as

$$\begin{aligned} \dot{x}(t) &= Ax(t) + Bu(t) = Ax(t) + Bu(t-L) = \begin{bmatrix} 0 & 1 \\ 0 & -3.784 \end{bmatrix} x(t) \\ &+ \begin{bmatrix} -1.892 \\ -0.786 \end{bmatrix} u(t-L) \end{aligned} \quad (26b)$$

By substuting in Riccati Eq. (10) to obtain positive definite solution to estimate gain matrix F ,

$$\begin{aligned} A^T P + PA - PBR^{-1}B^T + QC &= \begin{bmatrix} 0 & 1 \\ 0 & -8.317 \end{bmatrix}^T \begin{bmatrix} 1.277 & 0.375 \\ 0.293 & 1.342 \end{bmatrix} \\ &+ \begin{bmatrix} 1.277 & 0.375 \\ 0.293 & 1.342 \end{bmatrix} \\ &\quad \begin{bmatrix} 0 & 1 \\ 0 & -8.317 \end{bmatrix} \\ &- \begin{bmatrix} 1.277 & 0.375 \\ 0.293 & 1.342 \end{bmatrix} \begin{bmatrix} -0.914 \\ -1 \end{bmatrix} [1 \ 0 \ 0]^{-1} \begin{bmatrix} -0.914 \\ -1 \end{bmatrix}^T \\ &+ \begin{bmatrix} 4.321 & 2.973 \\ 0 & 3.246 \end{bmatrix} \begin{bmatrix} 1 & 0 \\ 0 & 1 \end{bmatrix} = 0 \end{aligned} \quad (27)$$

For Eq. (27), its positive analytical solutions of $P_{11} = 1.311$, $P_{12} = 0.823$, $P_{21} = 1.790$, $P_{22} = 1.372$ respectively. From these values, evaluating gain matrix $F = R^{-1}[P_{12} \ P_{22}]$.

$$F = [1 \ 0 \ 0]^{-1}[0.823 \ 1.790] = [3.642 \ 2.781 \ 0] \quad (28)$$

So the closed loop system matrix A_c of flow control loop in the lab-scale setup from Eq. (24) by taking inverse Laplace transform of Eq. (22), the following values are obtained

$$\exp(Ac t) = l^{-1}(sI - Ac)^{-1} = A - BF = \begin{bmatrix} 0 & d_1 \\ d_2 & d_3 \end{bmatrix} = \begin{bmatrix} 0 & 2.823 \\ 1.442 & 3.426 \end{bmatrix} \quad (29)$$

By substituting these performances index values in Eq. (25), the following designed PID controller structure for flow control loop is given as

$$u(t) = 4.934e(t) + 1.567 \int e(t)dt + 2.641de(t)/dt \quad (30)$$

Similarly the same procedure is followed to obtain the PID tuning values [16] for the pressure control loop and derived final structure is given as

$$u(t) = 0.841e(t) + 0.602 \int e(t)dt + 1.024de(t)/dt \quad (31)$$

From Eqs. (30) and (31), the corresponding values of k_c , k_i and k_d determined for pressure and flow control of a fluid transport system is given in Table 3.

To evaluate the performance of designed LQR-PID controller for local field control of pressure and flow rate of the fluid transported through the pipeline, conventional controllers like IMC-PID (Internal Mode Controller) [17,18] and ZN-PID (Ziegler Nichols) [19] controllers are considered. The corresponding PID tuning values of IMC-PID and

Table 3
LQR-PID controller parameters.

| Controller | Tuning parameters for pressure | | | Tuning parameters for flow rate | | |
|--------------------|--------------------------------|----------------------|------------------------|---------------------------------|----------------------|------------------------|
| | k_c | $k_i = (k_c/\tau_i)$ | $k_d = (k_c * \tau_d)$ | k_c | $k_i = (k_c/\tau_i)$ | $k_d = (k_c * \tau_d)$ |
| LQR-PID controller | 0.841 | 0.602 | 1.024 | 4.934 | 1.567 | 2.641 |

Table 4
Conventional controllers tuning parameters with values.

| Tuning rules | Pressure | | | Flow rate | | |
|--|----------|--------|-------|-----------|--------|-------|
| | k_c | k_i | k_d | k_c | k_i | k_d |
| ZN-PID controller | | | | | | |
| $k_c = \frac{arp}{\partial K_p}$; $a \in [1.2, 2]$; $\tau_i = 20$ | 1.896 | 1.501 | 0.303 | 1.849 | 0.4903 | 2.629 |
| and $\tau_d = 0.50$ | | | | | | |
| IMC-PID controller | | | | | | |
| $k_c = \frac{\alpha}{k_p(2\tau_i - \alpha + \theta)}$; $\tau_i = \alpha$; | 1.765 | 0.1385 | 0.791 | 1.896 | 0.5466 | 4.508 |
| $\tau_d = \tau_2$ | | | | | | |
| $\alpha = \tau \{1 - (1 - \frac{\alpha}{\tau})^2 e^{-\frac{\theta}{\tau}}$; | | | | | | |
| $\tau_c = 2\theta$ | | | | | | |

ZN-PID controllers are given in Table 4.

Where k_c is controller gain and τ_b τ_d indicates the integral and derivative gain.

4.3. Experimental analysis and results

The performance of validating LQR-PID controller with ZN-PID and IMC-PID [20–22] controllers to maintain flow and pressure in the fluid transportation system is analyzed in both simulation and real-time experimentation. A PID control block is introduced to afford closed loop feedback control action to compare the characterization of each tuning method taken for comparison.

4.3.1. Simulation results

In the simulation study, a MATLAB/SIMULINK block with PID controller is developed to investigate the performances of ZN-PID, LQR-PID and IMC-PID controllers by holding same peak of maximum uncertainty (M_s) value. In a process, it is better to have small IAE (Integral Absolute Error) and TV (Total Variation of the input). In simulation time, when the error indices gets reduced it leads to increase of TV and M_s value leads system to unstable state. But in LQR and IMC based tuning method, the advantage is that (M_s) level can be adjusted by τ_c parameter to afford enhanced control action with reduced error indices [23]. For pressure and flow control, to reach stable transient response M_s value of 1.26 is maintained during all operating points for controller performance comparison in MATLAB platform is given in Fig. 5.

4.3.2. Performance analyses for pressure and flow control loop of fluid transport system

The performance of ZN, IMC, and LQR-PID controller are investigated at required setpoint ranges in order to normalize transporting fluid pressure and flow rate in the pipeline. The obtained back transient response during simulation in MATLAB with 500 lph flow rate and 3 kg/cm² pressure operating point is investigated for the measuring time of 120 s duration are displayed in Figs. 6 and 7.

From the Figs. 6 and 7, it is confirmed that the LQR-PID controller possesses minimum duration of time of about 39.5 s and 41 s to settle on its operating set point with overshoot and maintains the steady state. Whereas IMC-PID and ZN-PID tuning methods provides maximum settling time of about 88 s and 82 s for flow rate and 116.37 s and 87.75 s

for pressure respectively. It describes that LQR-PID controller offers 16.72% of improved quality indices on comparing with ZN-PID and IMC-PID controllers. The overshoot and minimum TV value in the LQR-PID controller ensures that it reacts to the transport system in fast manner pointing high rise time in order to settle very quickly to incorporate with the given set point of pressure and flow rate.

4.3.3. Setpoint tracking for pressure and flow control loop

A set point tracking performance of LQR-PID controller at various set point ranges such as 0.4 and 1.5 kg/cm² for pressure and 900 and 1400 lph for the flow rate are evaluated and compared with ZN-PID and IMC-PID controllers. Figs. 8 and 9 enumerates the response obtained by LQR-PID controller settles at very minimum duration of 40 s with better robustness in accordance with the dynamic variation of control parameters. It maintains steady state with less peak as compared to ZN-PID controller and 2.19% error tolerance as compared with IMC-PID controller. Tables 5 and 6 shows attained performance criteria measures of LQR-PID controller comparing with IMC and ZN-PID controllers for various operating points. However, IMC and ZN-PID controllers produces response which reaches set point after very long duration of 116 s and 87 s respectively. Figs. 8 and 9 describes that LQR-PID controller attains 12.67% peak initially but reaches steady state with minimum error indices of 20.94% as compared with ZN-PID and IMC-PID controllers. Comparing to conventional controller, LQR-PID controller retains very minimum TV values assuring steady state output over the measuring period. This practical LQR-PID controller confirms robust closed loop control performance due to its capability of tracking errors in online [24].

4.3.4. Disturbance rejection test for pressure and flow control loop

The disturbance rejection characteristics of LQR, IMC and ZN-PID controller is evaluated in simulation study at the pressure of 2.1 kg/cm² and flow rate of 1300 lph. By introducing step disturbance in the way of increasing the pressure to 3 kg/cm² and flow rate to 1600 lph during the time interval between 100 and 150 s as shown in Figs. 10 and 11. From the analysis result, it is clearly noticed that only LQR-PID controller overcomes the disturbance to provide fast response in a short span of 15.62 s with less overshoot of 11.33% on comparing with ZN-PID controllers on pressure. The application of LQR-PID controller on flow control loop reveals the poor disturbance rejection of ZN-PID and IMC-PID controllers with very high value of TV where LQR-PID tolerates the disturbance with a short span of 24.5 s with minimum TV value of 4.32 for pressure and 13.92 for flow rate by enhanced quality indices. The performance measure regarding the disturbance rejection of the investigating controllers for pressure and flow rates are given in Table 7.

Hence by simulation results, LQR-PID controller contributes optimal smallest settling time with least error integral value and highest robustness on comparing with ZN-PID and IMC-PID controllers and hence affords 14.18% enhanced performance by comparing with quality indices of conventional controllers. It influences improved feedback control action in monitoring and maintaining the pressure and flow rate variations through the control valve opening and closing to obtain the desired operating range at the destination in the fluid transport system process plant.

5. Real-time experimental analysis of local intelligence

The LQR-PID controller performance is experimentally validated in real-time experimental scaled down-lab setup of the fluid transport system by analyzing with IMC, ZN-PID controllers through SCADA [25]. The resultant tuning values of PID controller using LQR technique is confirmed through simulation is put on to the created operator interface tune window using CENTUM VP. The fluid transport system is put to run by enabling the auto mode initiated by the operator when the set point for pressure and flow rate is given in the corresponding pressure

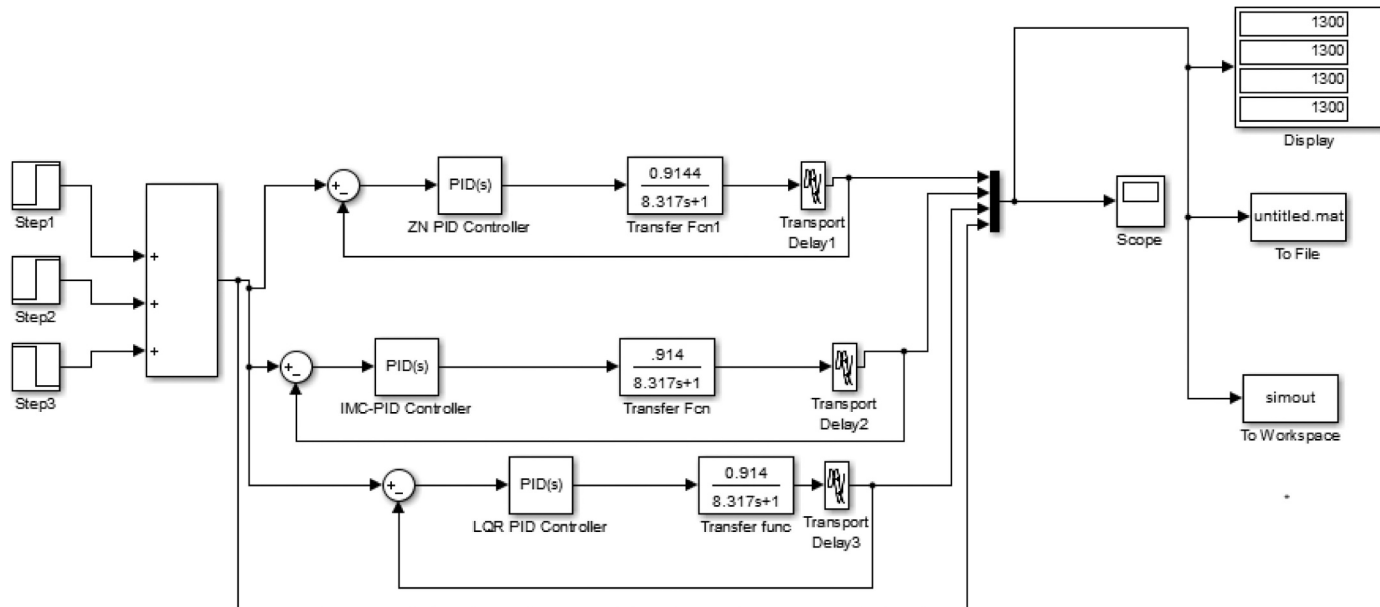


Fig. 5. MATLAB/SIMULINK model for pressure and flow control of fluid transport system.

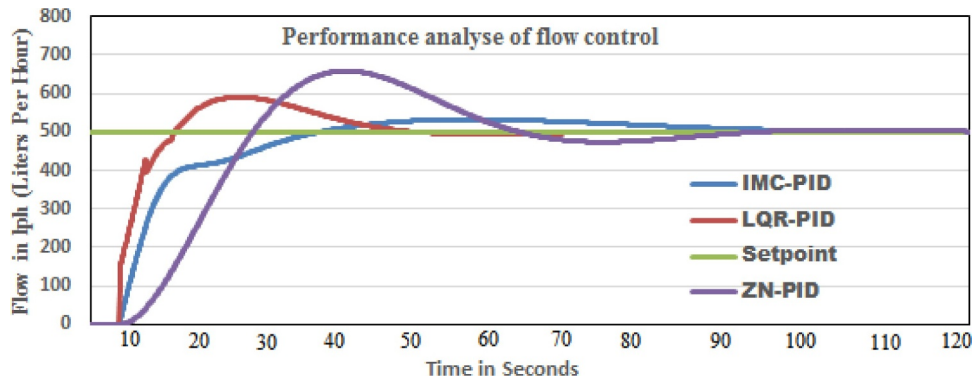


Fig. 6. Performance analyses of ZN-PID, IMC-PID, and LQR-PID controllers at a set point of 500 lph flow rate.

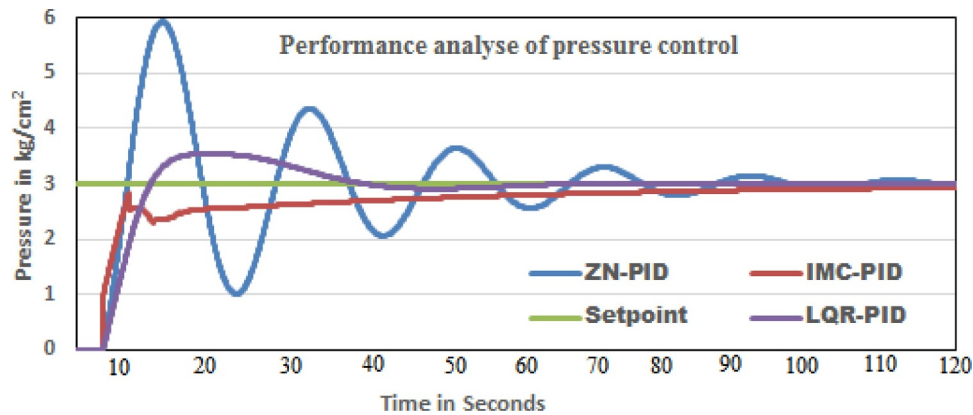


Fig. 7. Performance analyses of ZN-PID, IMC-PID, and LQR-PID controllers at a set point of 3 kg/cm² pressure.

and flow rate faceplate present in the SCADA front end panel. After fixing the required operating range, the pump will be on track to run which is enabled by an operator remotely [3]. The real-time successive data of both pressure and flow rate field parameters of the fluid transporting through pipeline is displayed continuously in created trend view window in PIC100.PV/ FIC100.PV tag tab which is present below the trend graph and these data can be exported to excel by enabling local utility data box option as shown in Fig. 12.

The real-time performance analyses by ZN, IMC and LQR-PID controller on monitoring and control of pressure and flow rate of the fluid transport system are conducted by fixing the setpoint of pressure and the flow rate is given as 1.2 kg/cm² and 800 lph respectively. The validated controller performances readings are taken along with controller output signals are shown in Figs. 13 and 14 and its corresponding time integral performance criteria are tabulated as seen in Table 8. Based on the operating set point of pressure and flow rate, the

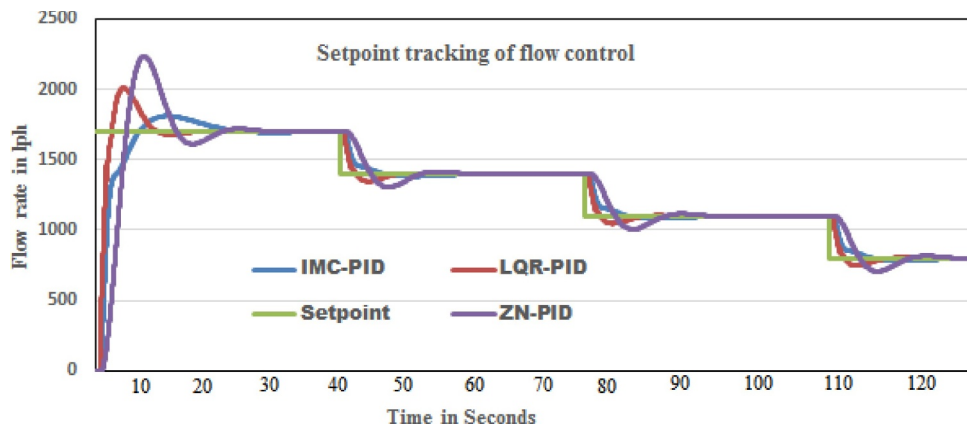


Fig. 8. Performance analyses of ZN-PID, IMC-PID, and LQR-PID controllers for flow control loop at various operating points.

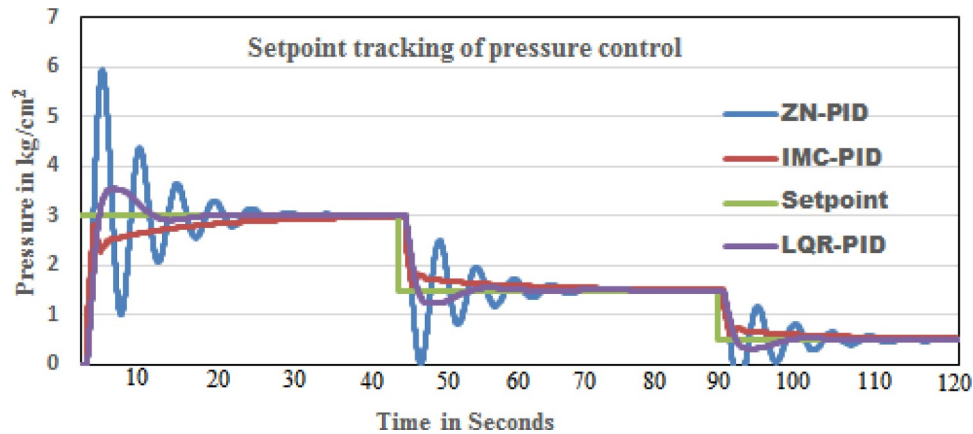


Fig. 9. Performance analyses of ZN-PID, IMC-PID, and LQR-PID controllers for pressure control loop at various operating points.

Table 5

Investigated controllers criteria measures for various set point of pressure.

| Operating points in kg/cm ² | Performance measures | ZN-PID | IMC-PID | LQR-PID |
|--|----------------------|----------|----------|-----------------|
| 0.4 | ISE | 0.00031 | 0.000435 | 0.001375 |
| | IAE | 0.0434 | 0.0405 | 0.037 |
| | ITAE | 0.1077 | 0.0749 | 0.04332 |
| | t_r (s) | 1.8 | 1.34 | 2.3 |
| | t_s (s) | 116.2 | 87.9 | 39.5 |
| | % M_p | 36.214 | 9.375 | 15.701 |
| 1.5 | TV | 15.97 | 12.25 | 6.88 |
| | ISE | 0.00031 | 0.000441 | 0.001375 |
| | IAE | 0.043426 | 0.040529 | 0.037077 |
| | ITAE | 0.107723 | 0.040529 | 0.037077 |
| | t_r (s) | 1.76 | 1.46 | 2.74 |
| | t_s (s) | 117.34 | 84.972 | 40.23 |
| 3 | % M_p | 36.347 | 11.782 | 17.931 |
| | TV | 15.73 | 11.98 | 6.43 |
| | ISE | 0.000344 | 0.000491 | 0.000253 |
| | IAE | 0.035908 | 0.024387 | 0.01444 |
| | ITAE | 0.014475 | 0.013514 | 0.012359 |
| | t_r (s) | 1.91 | 1.64 | 2.38 |
| | t_s (s) | 120.543 | 92.561 | 41.837 |
| | % M_p | 37.102 | 16.417 | 18.011 |
| | TV | 15.82 | 12.03 | 6.37 |

implemented controller running on the back end of the SCADA adjusts the feedback signal going from the remote master control panel to the I/P converter incorporated with a corresponding pressure control valve and flow control valve to regulate its opening and closing installed on the process plant control loops [12,16].

The real-time experimentation discloses that LQR-PID controller

Table 6

Investigated controllers criteria measures for various set point of flow rate.

| Operating points in lph | Performance measures | LQR-PID | IMC-PID | ZN-PID |
|-------------------------|----------------------|-----------------|----------|----------|
| 500 | ISE | 0.000417 | 0.00044 | 0.000435 |
| | IAE | 0.024718 | 0.027021 | 0.028951 |
| | ITAE | 0.036912 | 0.039539 | 0.047324 |
| | t_r (s) | 2.1 | 6.3 | 8.99 |
| | t_s (s) | 41.5 | 82.5 | 87.95 |
| | % M_p | 18.36 | 13.075 | 27.98 |
| 900 | TV | 13.82 | 17.26 | 19.57 |
| | ISE | 0.01667 | 0.0176 | 0.001741 |
| | IAE | 0.049436 | 0.054043 | 0.057901 |
| | ITAE | 0.029675 | 0.030249 | 0.030684 |
| | t_r (s) | 2.3 | 6.41 | 9.14 |
| | t_s (s) | 43 | 87.01 | 91.102 |
| 1400 | % M_p | 20.89 | 15.152 | 29.39 |
| | TV | 13.19 | 16.93 | 20.03 |
| | ISE | 0.01887 | 0.000356 | 0.018872 |
| | IAE | 0.024094 | 0.02658 | 0.025112 |
| | ITAE | 0.038954 | 0.042130 | 0.043897 |
| | t_r (s) | 2 | 5.98 | 8.93 |
| | t_s (s) | 42.84 | 86.12 | 84.89 |
| | % M_p | 14.57 | 14.936 | 27.134 |
| | TV | 13.97 | 17.3 | 19.84 |

accomplishes 26.2% better results than ZN, IMC-PID controller by comparing error indices in regulating control valve to maintain pressure and flow rate through the pipelines. Among the considered controller tunings, LQR-PID controller provides very minimum total variance value of 2.94 for pressure and 6.54 for flow confirming the smoothness and consistency of the generated output signal. When the

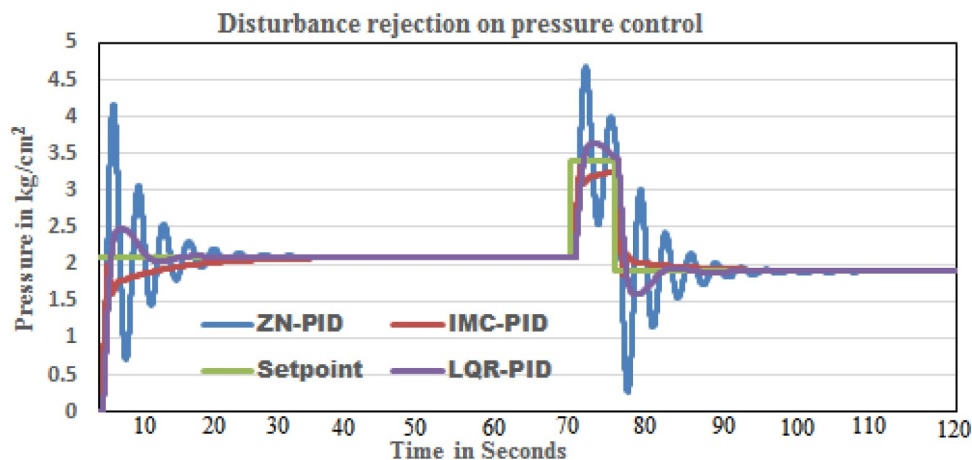


Fig. 10. Performance analyses of ZN-PID, IMC-PID, and LQR-PID controllers for pressure by a disturbance at a set point of $2.1 \text{ kg}/\text{cm}^2$.

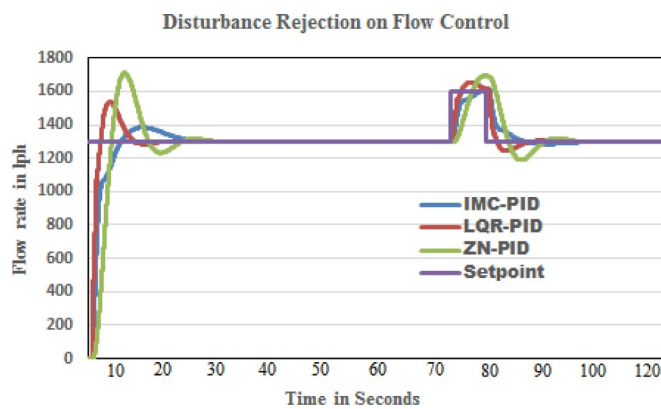


Fig. 11. Performance analyses of ZN-PID, IMC-PID, and LQR-PID controllers for flow by a disturbance at a set point of 1300 lph .

percentage of control valve opening gets increased, the field parameters such as pressure and flow rate of the fluids passing through the pipelines get decreases and increases consistently. The developed LQR-PID controllers confirm the enriched control behavior due to its interoperability and highest robustness to track error remotely when the fluid transport system gets called up through SCADA.

6. Results and discussions

The validated SCADA with LQR-PID controller monitors and controls field parameters such as pressure and flow rate in well regulated manner only when the pressure and flow rate variations are within safer operating range. But during, abnormal changes in the pressure and flow rate caused by pipeline failures, the developed local intelligences does not affords suitable control actions, hence it leads to serious risk occurrences. To resolve this issue, closed loop behavior of the local

intelligence is monitored and controlled through high level operating interface using IoT smart module. By continuously analyzing the receiving field sensors data in the cloud server, during crack and leakages in the pipelines immediately developed emergency shut off will be enabled from the central cloud server. The Fig. 15 shows the communication link established in the Integrated IoT architecture for fluid transportation system.

6.1. Smart IoT module for online monitoring and control

The proposed Integrated IoT architecture is practically experimented in fluid transport system by using the miniaturized breadboard design of the portable smart IoT module to acquire selected sensor data for concise monitoring and control purposes. The smart IoT module is a bond between embedded sensors and the control center, in which the communication can be achieved by employing RPL (Routing Protocol for Lossy networks) [25]. The complete hardware of smart IoT module is shown in Fig. 16.

The online server-based operator interface coordinates the field operations and cloud server communication simultaneously by running in a web platform accessed through portable devices with internet [27]. Through this web-oriented interface, the data retrieved from the cloud server are displayed in the form of JSON (JavaScript Object Notation) syntax. IoT front end is incorporated with MySQL database in the cloud server for storing the pressure and flow rate data respectively [30–34].

6.2. Emergency shut off configuration and interface with hardware setup

In IoT front end operator interface under fluid transport system only two parameters are taken for experimentation, the pressure transmitter data is labeled as IP1 and flow rate data is assigned as IP4. In the IoT smart module, the analog current input port of AC1 is configured to receive the pressure transmitter signal and AC4 is assigned to acquire flow transmitter data which is then transmitted to cloud for storage and

Table 7

Regulatory response of controllers at the operating point of pressure with $2.1 \text{ kg}/\text{cm}^2$ and flow rate of 1300 lph .

| Performance measures | Pressure | | | Flow rate | | |
|----------------------|----------|----------|-----------------|-----------------|----------|----------|
| | ZN-PID | IMC-PID | LQR-PID | LQR-PID | IMC-PID | ZN-PID |
| ISE | 0.000453 | 0.000418 | 0.000389 | 0.039257 | 0.043302 | 0.042816 |
| IAE | 0.014475 | 0.013514 | 0.012359 | 0.026801 | 0.028617 | 0.027843 |
| ITAE | 0.007482 | 0.008391 | 0.006453 | 0.0141 | 0.018 | 0.0268 |
| t_f (s) | 1.992 | 3.024 | 4.982 | 9.34 | 7.921 | 5.973 |
| t_s (s) | 39.02 | 48.13 | 19.02 | 20.137 | 34.856 | 52.465 |
| %M _p | 40.127 | 23.272 | 29.846 | 19.357 | 10.954 | 33.045 |
| TV | 10.59 | 8.61 | 4.32 | 13.92 | 17.66 | 20.17 |

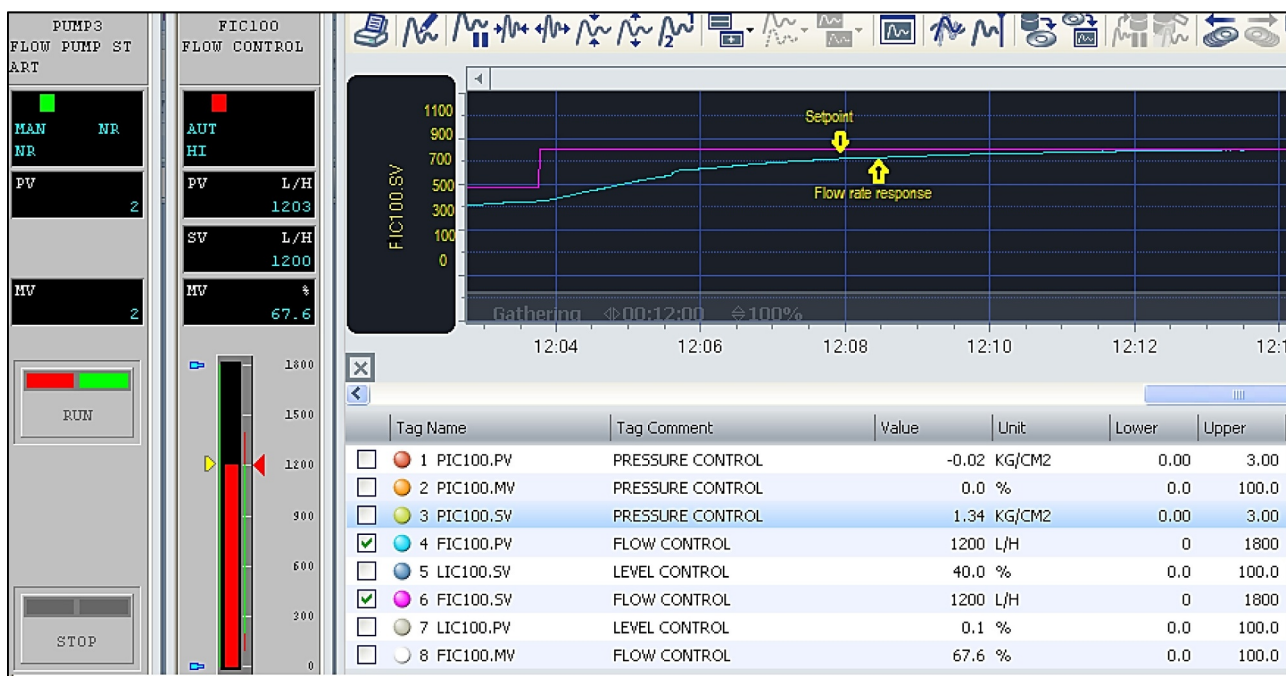


Fig. 12. Real-time monitoring and control of pressure and flow using a Local Intelligence at a field control station.

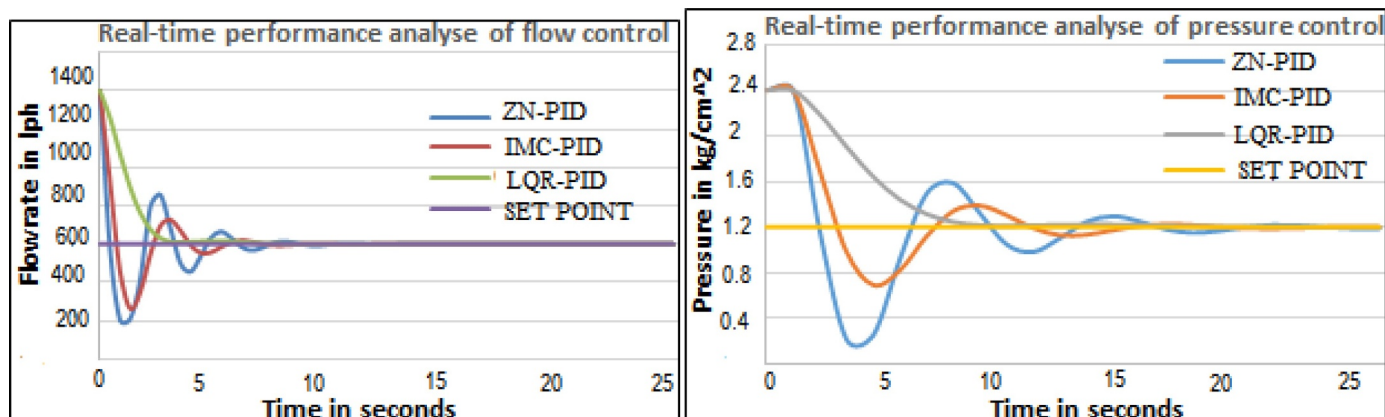


Fig. 13. Real-time performance analyses of pressure and flow rate using ZN, IMC and LQR-PID controller.

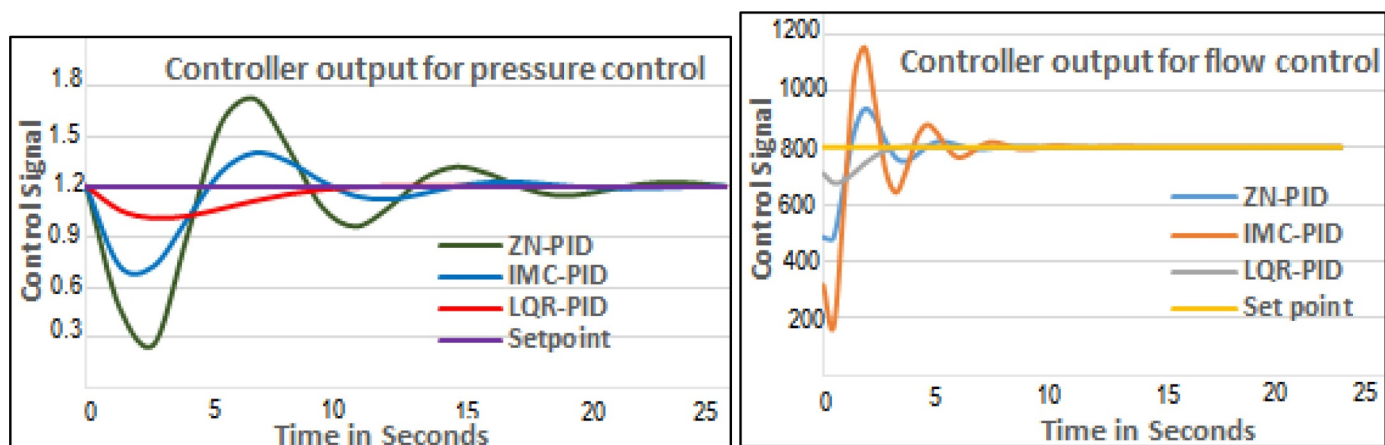


Fig. 14. Controllers output signals for pressure and flow control in the DCS fluid transportation system.

Table 8

Performance measures at the operating point of pressure at 1.2 kg/cm² and flow rate at 800 lph.

| Performance measures | Pressure | | | Flow rate | | |
|----------------------|----------|---------|---------------|----------------|---------|--------|
| | ZN-PID | IMC-PID | LQR-PID | LQR-PID | IMC-PID | ZN-PID |
| ISE | 0.0923 | 0.0798 | 0.0374 | 0.02347 | 0.0521 | 0.0752 |
| IAE | 0.0725 | 0.0427 | 0.0249 | 0.0193 | 0.0296 | 0.0341 |
| ITAE | 0.03114 | 0.0275 | 0.0136 | 0.00952 | 0.018 | 0.0127 |
| t_r (s) | 5.34 | 4.057 | 2.01 | 4.871 | 6.32 | 8.34 |
| t_s (s) | 24.02 | 19 | 12 | 10.27 | 12.621 | 18.241 |
| %M _p | 21.03 | 15.68 | Nil | Nil | 12.38 | 19.937 |
| TV | 7.73 | 5.82 | 2.94 | 6.54 | 10.14 | 13.21 |

analysis [28,29]. The digital output port of DO1 is programmed to get activated during an emergency shut off enabled condition. This DO1 digital output relay directly makes the interfaced pump to an off state by disabling the local intelligence functioning at the field station.

A SCADA is designed in such a way that the pump status can be available as either auto, manual, or stop mode [38,39]. Once the IoT module is interfaced, the pump status will be switched to auto mode automatically. A digital output port of DO1 is interfaced with the



Fig. 16. Smart IoT module complete hardware with its corresponding design notations.

output hub terminal station through which its triggering signal will be passed to engineering station to change the pump mode. When DO1 signal is received from the cloud, spontaneously the pump status will be changed to stop mode by proper engineering station command created for emergency shutoff through smart module. The local control unit with LQR-PID controller to be disengaged during this time. Based on the

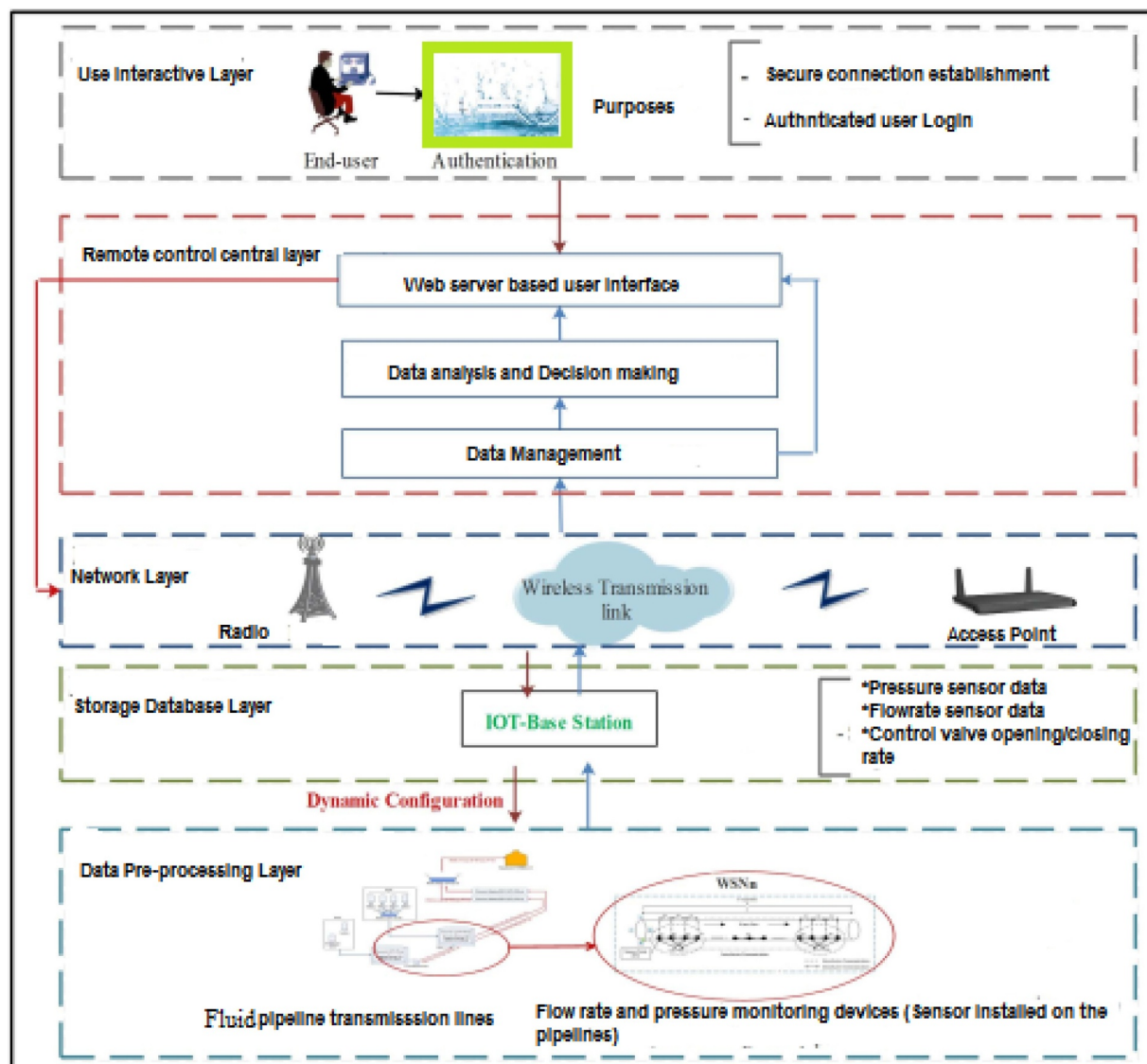


Fig. 15. Reliable integrated IoT architecture for online monitoring and control purpose.

Table 9
Configuration details of IoT module with hardware.

| Fluid transportation system | | |
|--|-------------------------|-----------|
| Manipulating parameters | Pressure 4 | Flow rate |
| Upper limit | 2.35 kg/cm ² | - |
| Lower limit | 0.15 kg/cm ² | - |
| Label notation in IoT front end | IP1 | IP4 |
| Input port configuration in IoT module | AC1 | AC4 |
| Emergency shutoff activating output port in IoT module | DO1 | |

real-time experimentation and analysis on the fluid transportation system, the corresponding pressure limit for the desired flow rate is well calibrated. **Table 9** gives the maximum and minimum limit for each manipulating pressure variable acquired from the pipeline field.

A high-level operator IoT interface continuously analyze each pressure data from the corresponding fluid pipeline concerning monitoring flow rate. For the undertaken transport setup, the status table is developed based on pressure rise and drop by crack in the fluid pipelines done manually to evaluate the pipeline system during abnormality. **Fig. 17** shows the established emergency shut off activation algorithm based on the real-time field pressure data of fluid pipeline system obtained during both normal and abnormal operating conditions.

By utilizing optimize table property, the condition table for the fluid transport system is created by taking the open loop response table enumerated in **Section 4** showing the respective pressure range for monitoring flow rate at the destination will be uploaded during the initial calibration of the database. In addition to the computing technique of pressure data with the condition table, it also checks the boundary limit

of received pressure data to activate the emergency shutoff by checking with the status table. If the deviation is within ± 0.65 , it will not affect the fluid pipeline system, but when the deviation exceeds or gets dropped from this tolerance rate, it shows the warning indication. Designed IoT front end message monitor points particular pressure label showing sudden pressure rise or drop to the operating engineer. The emergency shut off activation is different from comparison with the optimize table option. If assigned pressure label IP1 shows the pressure variation above 2.35 kg/cm² below 0.25 kg/cm² in the status table indicates the possibility of crack or leak in the fluid pipeline.

6.3. Experimental results of IoT smart module performance in fluid transport system at the abnormal operating condition

For validation of integrated IoT architecture, a manual hand valve is used to create a leak to ensure the performance of IoT module in the case of the abnormal situation caused by the cracks in the fluid pipelines. Initially, the smart module starts to communicate with the cloud by sending the pressure and flow rate data continuously. When the compare algorithm with status table executed in the MySQL database, the IoT front end notifies pressure drop of 0.19 kg/cm² in IP1 rather than to remain in the required pressure rate of 0.31 kg/cm². It displays warning notification for pressure drop at IP1 in the message monitor to the inspection engineer. Successively when it is checked with condition table of fluid transport system, for monitoring 1500 lph flow rate the lower limit should not reach below 0.25 kg/cm² but the received pressure data has attained a range of 0.19 kg/cm².

Hence instantly, emergency shut off is initiated by disabling local intelligence, as shown in **Fig. 18**. When the emergency shutoff is activated through a smart module via online in a lab-scale hardware setup. It enables the digital output port of DO1 connected with the input/

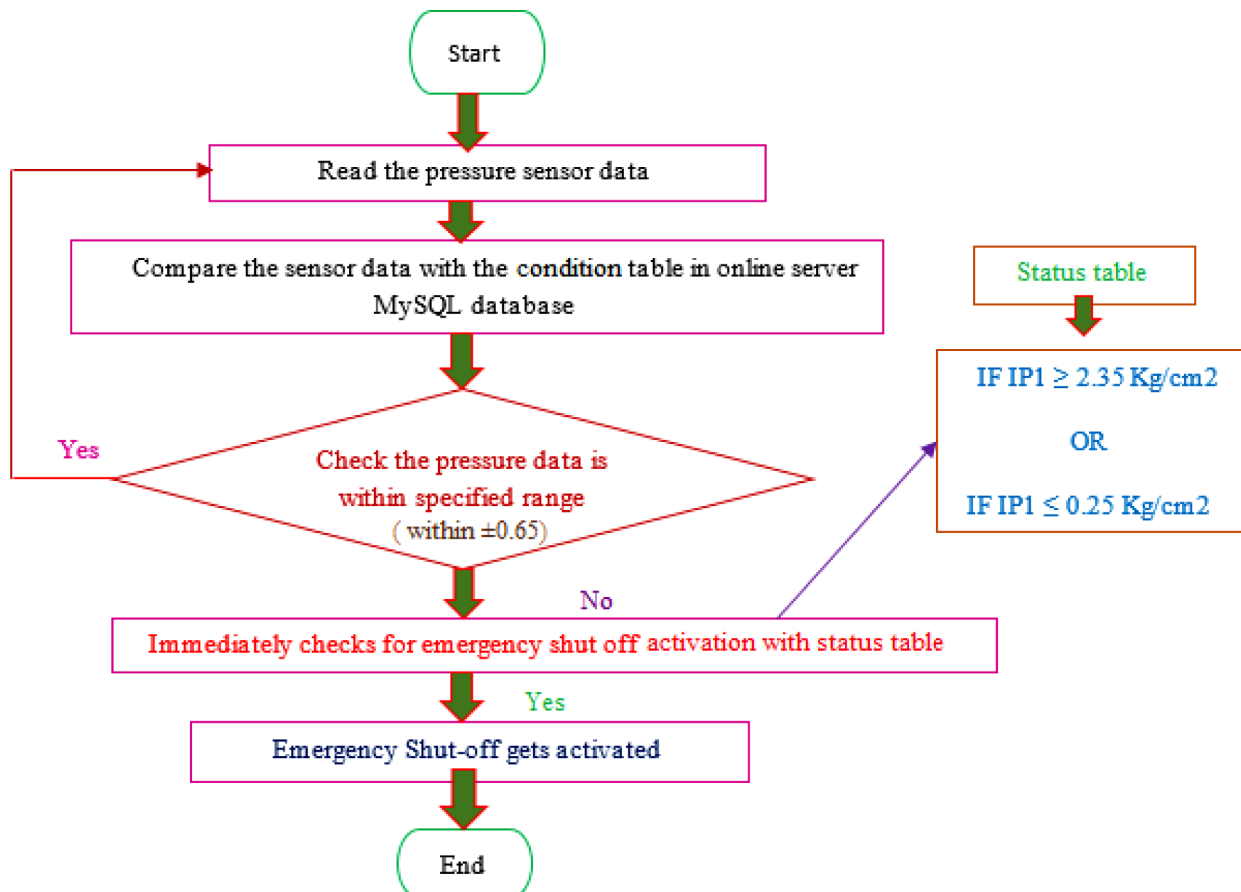


Fig. 17. Emergency shutoff execution algorithm for the fluid transport system via online.

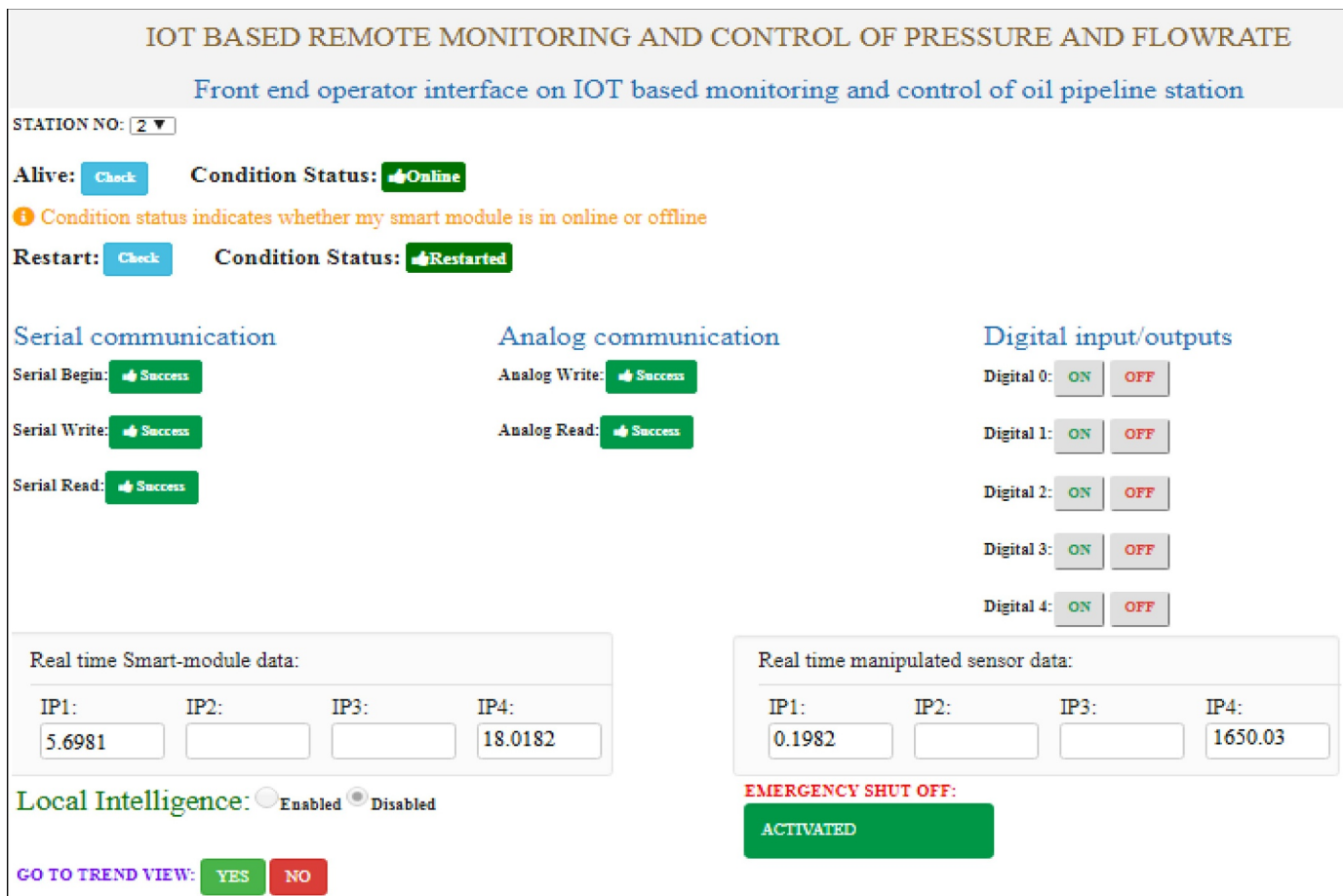


Fig. 18. IoT front end for the fluid pipeline system during the abnormal operating condition.

output hub terminal at field station. Once this DO1 activation signal is received at oil station 2, high-level engineering station sends the command signal to the SCADA to change the pump status from auto to stop mode. Simultaneously the engineering station disengages the LQR-PID controller from the output hub terminal. Hence the control function is stopped at the field station and the drain valve discharge the transported fluid in the pipeline to the process tank.

7. Conclusion and future scope

Based on the model identification to analyze the local intelligence performance, the corresponding optimal LQR-PID controller parameters ($K_c = 4.934$; $T_i = 1.567$ s; $T_D = 2.641$ s) were computed. Through the simulation results obtained for the 500 lph flow rate and 3 kg/cm² pressure, it confirms that the LQR-PID controller affords 14.18% enhanced performance by comparing quality indices in regulating the flow rate by adjusting control valve stem position. Based on performance analysis using MATLAB/Simulink, LQR-PID controller is used in real time experimental hardware. The real-time experimentation discloses that LQR-PID controller accomplishes 26.2% better results than ZN, IMC-PID controller by comparing error indices in regulating control valve to maintain pressure and flow rate. On comparing with ZN and IMC-PID controller, LQR-PID controller clearly emphasize the enhanced control performance possessing minimum settling time of 10.27 s with very small rise time of 4.87 s. LQR-PID controller provides very minimum total variance value of 2.94 for pressure and 6.54 for flow rate confirming the smoothness and consistency of the generated output signal to regulate control valve. Hence the implemented LQR-PID controllers confirm the better control action due to its interoperability and highest robustness at the local field station in maintaining the

pressure and flow rate of the fluid in the pipelines.

During cracks and leaks in the fluid pipelines, the developed main emergency shut off control in the cloud server gets activated by stopping the pumps when the local intelligence fails to respond at the appropriate time. Because through the online high-level engineering operator interface incorporated with smart IoT module, the assigned pressure labels should not exceed above 2.35 kg/cm² and not go below 0.25 kg/cm² range. When it encounters these pressure reaching situations, immediately emergency shut off gets activated. Also in the proposed architecture, the tolerance range of pressure variation should be within ± 0.65 deviation range on comparing with the required pressure range to maintain the desired flow rate in the fluid pipelines. Hence by the Integrated IoT based intelligent architecture with the local intelligence (LQR-PID controller with SCADA) ensures that the hardware configuration gets synchronized with the flexibility of smart IoT module to provide online monitoring and control capabilities from a remote location during leaks and cracks in the long range fluid pipelines.

Regarding the future work, the present experimented LQR-PID controller along with SCADA as a local intelligence in an Internet of Things (IoT) based reliable monitoring and control modular architecture will be implied real-time in the industrial oil pipeline system. Advanced machine learning algorithm will be applied for data analysis in order to identify anomaly occurrences on the process plant.

CRediT authorship contribution statement

E.B. Priyanka: Conceptualization, Formal analysis, Methodology, Data curation, Writing - original draft. **C. Maheswari:** Supervision. **S. Thangavel:** Software, Writing - review & editing. **M. Ponni Bala:** Formal analysis, Visualization.

Declaration of Competing Interest

The authors declare that they have no known competing financial interests or personal relationships that could have appeared to influence the work reported in this paper.

Acknowledgment

This research work is carried out under the Senior Research fellowship received from CSIR (Council for Scientific and Industrial Research) with grant no. 678/08(0001)2k18 EMR-I.

References

- [1] M. Meribout, A wireless sensor network based infrastructure for real-time and on-line pipeline inspection, *IEEE Sens. J.* 11 (11) (2011) 2966–2972.
- [2] R.C. Barros, M.F. Santos, A.F. Santos, M.F. Silva, V.F. Vidal, Monitoring platform, identification and control of level system based on SCADA architecture, *IEEE Trans. Ind. Electron.* 18 (2018) 283–288.
- [3] M. Abreu, D. Perez, K. Velasquez, M. Curado, E. Monteiro, A resilient Internet of Things architecture for smart cities, *Ann. Telecommun.* 72 (2016) 1–12.
- [4] E.B. Priyanka, C. Maheswari, S. Thangavel, Proactive decision making based iot framework for an oil pipeline transportation system, Proceedings of the International Conference on Computer Networks, Big Data and IoT, Springer, Cham, 2018, pp. 108–119.
- [5] P. Gawade, A. Meeankshi, IOT based smart public transport system, *Int. J. Sci. Res. Publ.* 7 (7) (2017) 390–396.
- [6] T. Subramanian, P. Bhaskaran, Local intelligence for remote surveillance and control of flow in fluid transportation system, *Adv. Model. Anal. C* 74 (1) (2019) 15–21, https://doi.org/10.18280/ama_c.740102.
- [7] E. Priyanka, C. Maheswari, M. Ponnibala, S. Thangavel, SCADA based remote monitoring and control of pressure & flow in fluid transport system using IMC-PID controller, *Adv. Syst. Sci. Appl.* 19 (3) (2019) 140–162, <https://doi.org/10.25728/assa.2019.19.3.676>.
- [8] J. Lloret, J. Tomas, A. Canovas, L. Parra, An integrated IoT architecture for smart metering, *IEEE Commun. Mag.* 54 (12) (2016) 50–57.
- [9] M. Morari, E. Zafiriou, Robust Process Control, Prentice Hall Englewood Cliffs, NJ, 1989.
- [10] D.E. Seborg, T.F. Edgar, D.A. Mellichamp, Process Dynamics and Control, 2nd ed., John Wiley & Sons, New York, USA, 2004.
- [11] G. Brendan, P. Gerhard, Introduction to industrial control networks, *IEEE Commun. Surv. Tutor.* 15 (2) (2013) 860 the second quarter of.
- [12] E. Priyanka, C. Maheswari, S. Thangavel, Remote monitoring and control of LQR-PI controller parameters for an oil pipeline transport system', Proceedings of the Institution of Mechanical Engineers, Part I, Journal of Systems and Control Engineering 233 (6) (2019) 597–608, <https://doi.org/10.1177/0959651818803183>.
- [13] J.B. He, W. Qing-Guo, L. Tong-Heng, PI/PID controller tuning via LQR approach, *Chem. Eng. Sci.* 55 (13) (2000) 2429–2439.
- [14] A. Hosseini Heidari, S. Etedali, M. Reza Javaheri-Tafti, A hybrid LQR-PID control design for seismic control of buildings equipped with ATMD, *Front. Struct. Civil Eng.* 12 (1) (2018) 44–57.
- [15] S. Das, P. Indranil, H. Kausik, S. Das, G. Amitava, LQR based improved discrete PID controller design via optimum selection of weighting matrices using fractional order integral performance index, *Appl. Math. Model.* 37 (6) (2013) 4253–4268.
- [16] J.K. Pradhan, G. Arun, MIMO PID controller design via linear quadratic regulator-linear matrix inequality approach, *IET Control Theory Appl.* 9 (14) (2015) 2401–2405.
- [17] L. Sangeetha, B. Naveen Kumar, A.B. Ganesh, N. Bharathi, Experimental validation of PID based cascade control system through SCADA-PLC-OPC and internet architectures, *Measurements* 41 (9) (2012) 789–795.
- [18] E.B. Priyanka, C. Maheswari, Parameter monitoring and control during petrol transportation using PLC based PID controller, *J. Appl. Res. Technol.* 14 (5) (2016) 125–131.
- [19] M. Shamsuzzoha, M. Lee, Analytical design of enhanced PID-filter controller for integrating and fist order unstable processes with time delay, *Chem. Eng. Sci.* 63 (2008) 2717–2731.
- [20] M. Shamsuzzoha, M. Lee, Enhanced disturbance rejection for an open-loop unstable process with time delay, *ISA Trans.* 48 (2009) 237–244.
- [21] E.B. Priyanka, C. Maheswari, S. Thangavel, Remote monitoring and control of an oil pipeline transportation system using a Fuzzy-PID controller, *Flow Meas. Instrum.* 62 (2018) 144–151.
- [22] W. Tan, H. Marquez, T. Chen, IMC design for unstable processes with time delays, *J. Process Control* 13 (2003) 203–213.
- [23] X. Yang, Q. Wang, C. Hang, C. Lin, IMC-based control system design for unstable processes, *Ind. Eng. Chem. Res.* 41 (2002) 4288–4294.
- [24] Y.V. Pavan Kumar, R. Bhimasingu, Key aspects of smart grid design for distribution system automation: architecture and responsibilities, *Proc. Technol.* 21 (2015) 352–359 ISSN 2212-0173.
- [25] K. El-Darymli, F. Khan, M.H. Mohammed, Reliability modeling of wireless sensor networks for oil and gas pipelines monitoring, *Sens. Transducers J.* 108 (7) (2014) 4122–4133.
- [27] L. Atzori, A. Iera, G. Morabito, M. Nitti, The Social Internet of Things (SIoT)—when social networks meet the internet of things: concept, architecture and network characterization, *Comput. Netw.* 56 (16) (2012) 3594–3608.
- [28] T. Strasser, F. Andrén, F. Lehfuss, M. Stifter, P. Palensky, Online reconfigurable control software for IEDs, *IEEE Trans. Ind. Inf.* 9 (3) (2017) 1455–1465.
- [29] W. Hu, Z. Lei, H. Zhou, G.-P. Liu, Q. Deng, D. Zhou, Z.-W. Liu, Plug-in free web-based 3-d interactive laboratory for control engineering education, *IEEE Trans. Ind. Electron.* 64 (5) (2017) 3808–3818.
- [30] S. Li, et al., 5 G Internet of Things: a survey, *J. Ind. Inf. Integr.* 10 (2018) 1–9.
- [31] C.T. (Angus) Lai, P.R. Jackson, W. Jiang, Shifting paradigm to service-dominant logic via Internet-of-Things with applications in the elevators industry, *J. Manag. Anal.* 4 (1) (2017) 35–54.
- [32] Y. Lu, Blockchain and the related issues: a review of current research Topics, *J. Manag. Anal.* 5 (4) (2018) 231–255.
- [33] Z. Bi, Y. Liu, J. Krider, J. Buckland, J. Smith, Real-time force monitoring of smart grippers for Internet of Things (IoT) applications, *J. Ind. Inf. Integr.* 11 (2018) 19–28.
- [34] Y. Chen, A survey on industrial information integration 2016–2019, *J. Ind. Integr. Manag.* (2020), <https://doi.org/10.1142/S2424862219500167> online published.
- [35] H. Cai, et al., IoT-based configurable information service platform for product lifecycle management, *IEEE Trans. Ind. Inf.* 10 (2) (2014) 1558–1567.
- [36] L. Jiang, et al., An iot oriented data storage framework in cloud computing platform, *IEEE Trans. Ind. Inf.* 10 (2) (2014) 1443–1451.
- [37] C. Zhang, Y. Chen, A review of research relevant to the emerging industry trends: industry 4.0, IoT, block chain, and business analytics, *J. Ind. Integr. Manag.* (2020), <https://doi.org/10.1142/S2424862219500192>.
- [38] A.G. Finogeev, A.A. Finogeev, Information attacks and security in wireless sensor networks of industrial SCADA systems, *J. Ind. Inf. Integr.* 5 (2017) 6–16.
- [39] A.R. Panda, D. Mishra, H.K. Rathna, Implementation of SCADA/HMI system for real-time controlling and performance monitoring of SDR based flight termination system, *J. Ind. Inf. Integr.* 3 (2016) 20–30.
- [40] I.S.Pereira Renata, M.Dupont Ivonne, C.M.Carvalho Paulo, C.S.Jucá Sandro, IoT embedded linux system based on Raspberry Pi applied to real-time cloud monitoring of a decentralized photovoltaic plant, *Measurement* 114 (2018) 286–297.
- [41] D.E. Seborg, A.M. Duncan, F.E. Thomas, J.D. Francis III, Process dynamics and control, John Wiley & Sons, 2010.
- [42] L.M. Argentim, C.R. Willian, E.S. Paulo, A.A. Renato, PID, LQR and LQR-PID on a quadcopter platform, 2013 International Conference on Informatics, Electronics and Vision (ICIEV), IEEE, 2013, pp. 1–6.
- [43] C.T. Lai, P.R. Jackson, W. Jiang, Shifting paradigm to service-dominant logic via Internet-of-Things with applications in the elevators industry, *J. Manag. Anal.* 4 (1) (2017) 35–54.
- [44] C. Qing, Z. Wang, L. Zheng, B. Wu, Y. Wang, Shock wave approach for estimating queue length at signalized intersections by fusing data from point and mobile sensors, *Transp. Res. Rec.* 2422 (1) (2014) 79–87.
- [45] B.S. Suh, J.H. Yang, A tuning of PID regulators via LQR approach, *J. Chem. Eng. Jpn.* 38 (5) (2005) 344–356.